Chapter 17

Subtraction at NNLO and Higgs boson production at hadron colliders

M. Grazzini

17.1 Introduction

The dynamics of hard scattering processes involving hadrons is nowadays remarkably well described by perturbative QCD predictions. Thanks to asymptotic freedom, the cross section for sufficiently inclusive reactions can be computed as a series expansion in the QCD coupling α_S. Until few years ago, the standard for such calculations was next-to-leading order (NLO) accuracy. Next-to-next-to-leading order (NNLO) results were known only for few highly-inclusive reactions (see e.g. Refs. [1, 2, 3]).

The extension from NLO to NNLO accuracy is important to improve QCD predictions and to better assess their uncertainties. In particular, this extension is essential in two cases: in those processes whose NLO corrections are comparable to the leading order (LO) contribution; in those 'benchmark' processes that are measured with high experimental precision. Such a task, however, implies finding methods and techniques to cancel the infrared (IR) divergences that appear at intermediate steps of the calculations.

Recently, a new general method [4], based on sector decomposition [5], has been proposed and applied to the NNLO QCD calculations of $e^+e^- \to 2$ jets [6], Higgs [7] and vector [8] boson production in hadron collisions, and to the NNLO QED calculation of the electron energy spectrum in muon decay [9].

The calculations of Refs. [7, 8] allow us to compute the corresponding cross sections with arbitrary cuts on the momenta of the partons produced in the final state.

The traditional approach to perform NLO computations is based on the introduction of auxiliary cross sections that are obtained by approximating the QCD scattering amplitudes in the relevant IR (soft and collinear) limits. This strategy led to the proposal of the *subtraction* [10] and *slicing* [11] methods. Exploiting the universality properties of soft and collinear emission, these methods were later developed in the form of general algorithms [12, 13, 14]. that make possible to perform NLO calculations in a (relatively) straightforward manner, once the corresponding QCD amplitudes are available. In recent years, several research groups have been working on general NNLO extensions of the subtraction method [15, 16, 17, 18, 19]. Results have been obtained in some specific processes: $e^+e^- \to 2$ jets [20, 21] and, more recently, $e^+e^- \to 3$ jets [22, 23].

In Ref. [24] we proposed an extension of the subtraction method to NNLO for a specific, though important, class of processes: the production of colourless high-mass systems in hadron collisions. We presented a formulation of the subtraction method for this class of processes, and we applied it to the NNLO calculation of Higgs boson production via the gluon fusion subprocess $gg \to H$. The calculation has now been implemented in the numerical program `HNNLO`, which includes all the relevant decay modes of the Higgs boson for this production subprocess, namely, $H \to \gamma\gamma$ [24], $H \to WW \to l\nu l\nu$ and $H \to ZZ \to 4l$ [25].

This contribution is organized as follows. In Sect. 17.2 we discuss the version of the subtraction formalism we use. In Sect. 17.3 we present a selection of numerical results that can be obtained by our program. In Sect. 17.4 we summarize our results.

17.2 The method

We consider the inclusive hard-scattering reaction

$$h_1 + h_2 \to F(Q) + X, \tag{17.1}$$

where the collision of the two hadrons h_1 and h_2 produces the triggered final state F. The final state F consists of one or more colourless particles (leptons, photons, vector bosons, Higgs bosons, ...) with momenta q_i and total invariant mass Q . Note that, since F is colourless, the LO partonic subprocess is either $q\bar{q}$ annihilation, as in the case of the Drell–Yan process, or gg fusion, as in the case of Higgs boson production.

At NLO, two kinds of corrections contribute: i) *real* corrections, where one parton recoils against F; ii) *one-loop virtual* corrections to the LO subprocess. Both contributions are separately IR divergent, but the divergences cancel in the sum. At NNLO, three kinds of corrections must be considered: i) *double real* contributions, where two partons recoil against F; ii) *real-virtual* corrections, where one parton recoils against F at one-loop order; iii) *two-loop virtual* corrections to the LO subprocess. The three contributions are still separately divergent, and the calculation has to be organized so as to explicitly achieve the cancellation of the IR divergences.

Our method is based on a generalization of the procedure used in the specific NNLO calculation of Ref. [26]. We first note that, at LO, the transverse momentum $\mathbf{q}_T$ of the triggered final state F is exactly zero. As a consequence, as long as $q_T \neq 0$, the (N)NLO contributions are actually given by the (N)LO contributions to the triggered final state F + jet(s). Thus, we can write the cross section as

$$d\sigma^F_{(N)NLO}|_{q_T\neq 0} = d\sigma^{F+\text{jets}}_{(N)LO} \ . \tag{17.2}$$

This means that, when $q_T \neq 0$, the IR divergences in our NNLO calculation are those in $d\sigma^{F+\text{jets}}_{NLO}$: they can be handled and cancelled by using available NLO formulations of the subtraction method. The only remaining singularities of NNLO type are associated to the limit $q_T \to 0$, and we treat them by an additional subtraction. Our key point is that the singular behaviour of $d\sigma^{F+\text{jets}}_{(N)LO}$ when $q_T \to 0$ is well known: it appears in the resummation program [27, 28, 29] of logarithmically-enhanced contributions to transverse-momentum distributions. Then, to perform the additional subtraction, we follow the formalism used in Ref. [30, 31] to combine resummed and fixed-order calculations.

We use a shorthand notation that mimics the notation of Ref. [30]. We define the subtraction counterterm[1]

$$d\sigma^{CT} = d\sigma^F_{LO} \otimes \Sigma^F(q_T/Q)\, d^2\mathbf{q}_T. \tag{17.3}$$

The function $\Sigma^F(q_T/Q)$ embodies the singular behaviour of $d\sigma^{F+\text{jets}}$ when $q_T \to 0$. In this limit it can be expressed as follows in terms of q_T-independent coefficients $\Sigma^{F(n;k)}$:

$$\Sigma^F(q_T/Q) \xrightarrow[q_T\to 0]{} \sum_{n=1}^{\infty} \left(\frac{\alpha_S}{\pi}\right)^n \sum_{k=1}^{2n} \Sigma^{F(n;k)} \, \frac{Q^2}{q_T^2} \ln^{k-1}\frac{Q^2}{q_T^2} \ . \tag{17.4}$$

[1]The symbol $\otimes$ understands convolutions over momentum fractions and sum over flavour indeces of the partons.

The extension of Eq. (17.2) to include the contribution at $q_T = 0$ is finally:

$$d\sigma^F_{(N)NLO} = \mathcal{H}^F_{(N)NLO} \otimes d\sigma^F_{LO} + \left[d\sigma^{F+\text{jets}}_{(N)LO} - d\sigma^{CT}_{(N)LO} \right] \quad . \tag{17.5}$$

Comparing with the right-hand side of Eq. (17.2), we have subtracted the truncation of Eq. (17.3) at (N)LO and added a contribution at $q_T = 0$ needed to obtain the correct total cross section. The coefficient $\mathcal{H}^F_{(N)NLO}$ does not depend on q_T and is obtained by the (N)NLO truncation of the perturbative function

$$\mathcal{H}^F = 1 + \frac{\alpha_S}{\pi} \mathcal{H}^{F(1)} + \left(\frac{\alpha_S}{\pi} \right)^2 \mathcal{H}^{F(2)} + \dots \quad . \tag{17.6}$$

The counterterm of Eq. (17.3) regularizes the singularity of $d\sigma^{F+\text{jets}}$ when $q_T \to 0$: the term in the square bracket on the right-hand side of Eq. (17.5) is thus IR finite (or, better, integrable over q_T). Note that, at NNLO, $d\sigma^{CT}_{(N)LO}$ acts as a counterterm for the *sum* of the two contributions to $d\sigma^{F+\text{jets}}$: the *double real* plus *real-virtual* contributions. We also note that the counterterm function $\Sigma^F(q_T/Q)$ can be defined in different ways: the only property we require is that in the small q_T limit it must take the form given in Eq. (17.4), so as to match the singular behaviour of $d\sigma^{F+\text{jets}}$. Note that the perturbative coefficients $\Sigma^{F(n;k)}$ are universal: more precisely, the NNLO coefficients $\Sigma^{F(2;1)}$ and $\Sigma^{F(2;2)}$ have a non-universal contribution that, nonetheless, is proportional to the NLO coefficient $\mathcal{H}^{F(1)}$. The above coefficients only depend on the type of partons (quarks or gluon) involved in the LO partonic subprocess ($q\bar{q}$ annihilation or gg fusion). We finally note that the simplicity of the LO subprocess is such that final-state partons actually appear only in the term $d\sigma^{F+\text{jets}}$ on the right-hand side of Eq. (17.5). Therefore, arbitrary IR-safe cuts on the jets at (N)NLO can effectively be accounted for through a (N)LO computation. Owing to this feature, our NNLO extension of the subtraction formalism is observable-independent.

At NLO (NNLO), the physical information of the *one-loop (two-loop) virtual* correction to the LO subprocess is contained in the coefficients $\mathcal{H}^{(1)}$ ($\mathcal{H}^{(2)}$). Once an explicit form of Eq. (17.3) is chosen, the hard coefficients $\mathcal{H}^{F(n)}$ are uniquely identified (a different choice would correspond to different $\mathcal{H}^{F(n)}$). According to Eq. (17.5), the NLO calculation of $d\sigma^F$ requires the knowledge of $\mathcal{H}^{F(1)}$ and the LO calculation of $d\sigma^{F+\text{jets}}$. The general (process-independent) form of the coefficient $\mathcal{H}^{F(1)}$ is basically known: the precise relation between $\mathcal{H}^{F(1)}$ and the IR finite part of the one-loop correction to a generic LO subprocess is explicitly derived in Ref. [32].

At NNLO, the coefficient $\mathcal{H}^{F(2)}$ is also needed, together with the NLO calculation of $d\sigma^{F+\text{jets}}$. The coefficients $\mathcal{H}^{H(2)}$ for Higgs boson production in the large-M_{top} limit have been computed [33]. Since the NLO corrections

to $gg \to H + \text{jet(s)}$ are available [34] in the same limit, we are able to apply Eq. (17.5) at NNLO. We have encoded our computation in a parton level Monte Carlo program, in which we can implement arbitrary IR-safe cuts on the final state.

17.3 Results

In the following we present numerical results for Higgs boson production at the LHC. We use the MRST2004 parton distributions [35], with densities and α_S evaluated at each corresponding order (i.e., we use $(n+1)$-loop α_S at $\mathrm{N}^n\mathrm{LO}$, with $n = 0, 1, 2$). The renormalization and factorization scales are fixed to the value $\mu_R = \mu_F = M_H$, where M_H is the mass of the Higgs boson.

17.3.1 $H \to \gamma\gamma$

We consider the Higgs boson decay in the $H \to \gamma\gamma$ channel and follow Ref. [36] to apply cuts on the photons. For each event, we classify the photon transverse momenta according to their minimum and maximum value, $p_{T\min}$ and $p_{T\max}$. The photons are required to be in the central rapidity region, $|\eta| < 2.5$, with $p_{T\min} > 35$ GeV and $p_{T\max} > 40$ GeV. We also require the photons to be isolated: the hadronic (partonic) transverse energy in a cone of radius $R = 0.3$ along the photon direction has to be smaller than 6 GeV. When $M_H = 125$ GeV, by applying these cuts the impact of the NNLO corrections on the NLO total cross section is reduced from 19% to 11%. In Fig. 17.1 we plot the distributions in $p_{T\min}$ and $p_{T\max}$ for the $gg \to H \to \gamma\gamma$ signal. We note that the shape of these distributions sizeably differs when going from LO to NLO and to NNLO. The origin of these perturbative instabilities is well known [37]. Since the LO spectra are kinematically bounded by $p_T \leq M_H/2$, each higher-order perturbative contribution produces (integrable) logarithmic singularities in the vicinity of that boundary. More detailed studies are necessary to assess the theoretical uncertainties of these fixed-order results and the relevance of all-order resummed calculations.

In Fig. 17.2 we consider the (normalized) distribution in the variable $\cos\theta^*$, where θ^* is the polar angle of one of the photons in the rest frame of the Higgs boson. At small values of $\cos\theta^*$ the distribution is quite stable with respect to higher order QCD corrections. We also note that the LO distribution vanishes beyond the value $\cos\theta^*_{\max} < 1$. The upper bound $\cos\theta^*_{\max}$ is due to the fact that the photons are required to have a minimum p_T of 35 GeV. As in the case of Fig. 17.1, in the vicinity of this LO kinematical boundary there is an instability of the perturbative results beyond LO.

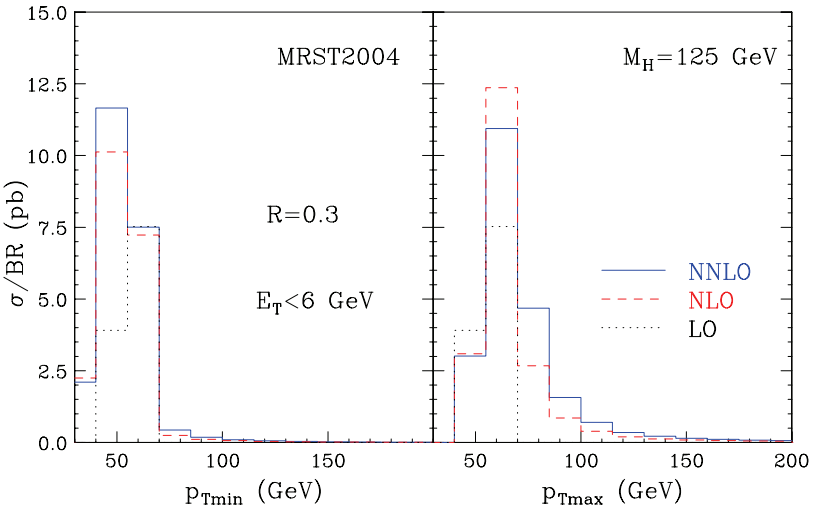

Figure 17.1: *Distributions in $p_{T\min}$ and $p_{T\max}$ for the diphoton signal at the LHC. The cross section is divided by the branching ratio in two photons.*

17.3.2 $H \to WW \to l\nu l\nu$

We now consider the production of a Higgs boson with mass $M_H = 165$ GeV in the decay mode $H \to WW \to l\nu l\nu$ [25]. We apply a set of selection cuts taken from the study of Ref. [38]. The charged leptons are classified according to their minimum and maximum p_T. The $p_{T\min}$ should be larger than 25 GeV, and $p_{T\max}$ should be between 35 and 50 GeV. The charged lepton rapidity should fullfil $|\eta| < 2$. The missing p_T of the event is required to be larger than 20 GeV and the invariant mass of the charged leptons is smaller than 35 GeV. The azimuthal separation of the charged leptons in the transverse plane ($\Delta\phi$) is smaller than 45^o. Finally, there should be no jet with $p_T^{\rm jet}$ larger than $p_T^{\rm veto}$ [2].

In Table 17.1 we report the corresponding cross sections in the case of $p_T^{\rm veto} = 30$ GeV.

The cuts are quite hard, the efficiency being 8% at NLO and 6% at NNLO. The scale dependence of the result is strongly reduced at NNLO, being of the order of the error from the numerical integration. The impact of higher order corrections is also drastically changed. The K-factor is now 1.19 at NLO and

[2] Jets are reconstructed with the k_T algorithm [39] with jet size $D = 0.4$.

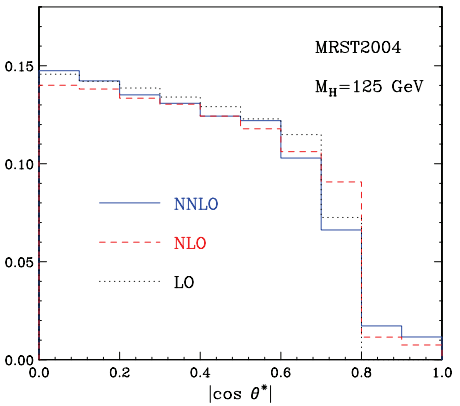

Figure 17.2: Normalized distribution in the variable $\cos\theta^*$.

σ (fb)	LO	NLO	NNLO
$\mu_F = \mu_R = M_H/2$	17.36 ± 0.02	18.11 ± 0.08	15.70 ± 0.32
$\mu_F = \mu_R = M_H$	14.39 ± 0.02	17.07 ± 0.06	15.99 ± 0.23
$\mu_F = \mu_R = 2M_H$	12.00 ± 0.02	15.94 ± 0.05	15.68 ± 0.20

Table 17.1: *Cross sections for* $pp \to H + X \to WW + X \to l\nu l\nu + X$ *at the LHC when selection cuts are applied and* $p_T^{\rm veto} = 30$ *GeV.*

1.11 at NNLO. As expected, the jet veto tends to stabilize the perturbative expansion, and the NNLO cross section turns out to be smaller than the NLO one.

17.3.3 $H \to ZZ \to e^+e^-e^+e^-$

We now consider the production of a Higgs boson with mass $M_H = 200$ GeV [25]. In this mass region the dominant decay mode is $H \to ZZ \to 4$ leptons, providing a clean four lepton signature. In the following we consider the decay of the Higgs boson in two identical lepton pairs. When no cuts are applied, the NLO K-factor is $K = 1.87$ whereas at NNLO we have $K = 2.26$. We find that the interference contribution is smaller than 1% in this region of Higgs boson masses.

We consider the following cuts [36]:

1. For each event, we order the transverse momenta of the leptons from the largest (p_{T1}) to the smallest (p_{T4}). They are required to fulfil the following thresholds:
   $p_{T1} > 30$ GeV $\quad p_{T2} > 25$ GeV $\quad p_{T3} > 15$ GeV $\quad p_{T4} > 7$ GeV;
2. Leptons should be central: $|y| < 2.5$;
3. Leptons should be isolated: the total transverse energy E_T in a cone of radius 0.2 around each lepton should fulfil $E_T < 0.05\ p_T$;
4. For each possible e^+e^- pair, the closest (m_1) and next-to-closest (m_2) to M_Z are found. Then m_1 and m_2 are required to be 81 GeV $< m_1 <$ 101 GeV and 40 GeV $< m_2 <$ 110 GeV.

These cuts are designed to maximize the statistical significance for an early discovery, but to keep the possibility for a more detailed analysis of the properties of the Higgs boson. The corresponding cross sections are reported in Table 17.2.

σ (fb)	LO	NLO	NNLO
$\mu_F = \mu_R = M_H/2$	1.541 ± 0.002	2.764 ± 0.005	3.013 ± 0.023
$\mu_F = \mu_R = M_H$	1.264 ± 0.001	2.360 ± 0.003	2.805 ± 0.015
$\mu_F = \mu_R = 2M_H$	1.047 ± 0.001	2.044 ± 0.003	2.585 ± 0.010

Table 17.2: *Cross sections for $pp \to H + X \to ZZ + X \to e^+e^-e^+e^- + X$ at the LHC when cuts are applied.*

Contrary to what happens in the $H \to WW \to l\nu l\nu$ decay mode, the cuts are quite mild, the efficiency being 63% at NLO and 62% at NNLO. The NLO and NNLO K-factors are 1.87 and 2.22, respectively. Comparing with the inclusive case, we conclude that these cuts do not change significantly the impact of QCD radiative corrections. We also find that the effect of lepton isolation is mild: at NNLO it reduces the accepted cross section by about 4%.

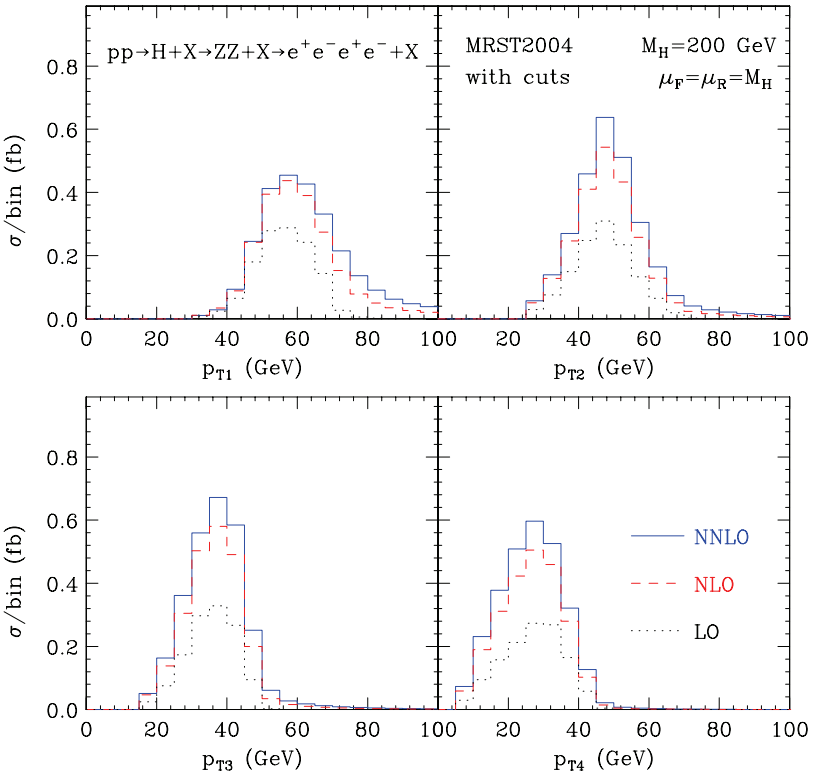

Figure 17.3: *Tranverse momentum spectra of the final state leptons for* $pp \to H + X \to ZZ + X \to e^+e^-e^+e^- + X$*, ordered according to decreasing* p_T*, at LO (dotted), NLO (dashed), NNLO (solid).*

In Fig. 17.3 we report the p_T spectra of the charged leptons. We note that at LO, without cuts, the p_{T1} and p_{T2} are kinematically bounded by $M_H/2$, whereas $p_{T3} < M_H/3$ and $p_{T4} < M_H/4$. Contrary to what happens in the $H \to \gamma\gamma$ decay mode (see Sect. 17.3.1) the distributions smoothly reach the

kinematical boundary, and no perturbative instability is observed beyond LO.

17.4 Summary

We have illustrated an extension of the subtraction formalism to compute NNLO QCD corrections to the production of high-mass systems in hadron collisions. We have considered an explicit application of our method to the NNLO computation of $gg \to H$ at the LHC, including the decay of the Higgs boson in all the relevant decay modes, namely, $H \to \gamma\gamma$, $H \to WW \to l\nu l\nu$ and $H \to ZZ \to 4$ leptons. We have presented few selected results, including kinematical cuts on the final state. In the case of the $H \to \gamma\gamma$ and $H \to WW \to l\nu l\nu$ decay modes, our computation parallels the one of Refs. [7, 40], but it is performed with a completely independent method. In the quantitative studies that we have carried out, the two computations give results in numerical agreement. In our approach the calculation is directly implemented in a parton level event generator. This feature makes it particularly suitable for practical applications to the computation of distributions in the form of bin histograms. The calculation is implemented in the numerical program `HNNLO`, which can be downloaded from [41].

References

1. S. G. Gorishnii, A. L. Kataev and S. A. Larin, Phys. Lett. B **259** (1991) 144; L. R. Surguladze and M. A. Samuel, Phys. Rev. Lett. **66** (1991) 560 [Erratum-ibid. **66** (1991) 2416]; K. G. Chetyrkin, Phys. Lett. B **391** (1997) 402.

2. R. Hamberg, W. L. van Neerven and T. Matsuura, Nucl. Phys. B **359** (1991) 343 [Erratum-ibid. B **644** (2002) 403]; E. B. Zijlstra and W. L. van Neerven, Nucl. Phys. B **383** (1992) 525; E. B. Zijlstra and W. L. van Neerven, Phys. Lett. B **297** (1992) 377.

3. R. V. Harlander and W. B. Kilgore, Phys. Rev. Lett. **88** (2002) 201801; C. Anastasiou and K. Melnikov, Nucl. Phys. B **646** (2002) 220; V. Ravindran, J. Smith and W. L. van Neerven, Nucl. Phys. B **665** (2003) 325.

4. C. Anastasiou, K. Melnikov and F. Petriello, Phys. Rev. D **69** (2004) 076010.

5. T. Binoth and G. Heinrich, Nucl. Phys. B **585** (2000) 741, Nucl. Phys. B **693** (2004) 134; K. Hepp, Commun. Math. Phys. **2** (1966) 301.

6. C. Anastasiou, K. Melnikov and F. Petriello, Phys. Rev. Lett. **93** (2004) 032002.

7. C. Anastasiou, K. Melnikov and F. Petriello, Phys. Rev. Lett. **93** (2004) 262002, Nucl. Phys. B **724** (2005) 197.

8. K. Melnikov and F. Petriello, Phys. Rev. Lett. **96** (2006) 231803, Phys. Rev. D **74** (2006) 114017.

9. C. Anastasiou, K. Melnikov and F. Petriello, arXiv:hep-ph/0505069.

10. R. K. Ellis, D. A. Ross and A. E. Terrano, Nucl. Phys. B **178** (1981) 421.

11. K. Fabricius, I. Schmitt, G. Kramer and G. Schierholz, Z. Phys. C **11** (1981) 315.

12. W. T. Giele and E. W. N. Glover, Phys. Rev. D **46** (1992) 1980; W. T. Giele, E. W. N. Glover and D. A. Kosower, Nucl. Phys. B **403** (1993) 633.

13. S. Frixione, Z. Kunszt and A. Signer, Nucl. Phys. B **467** (1996) 399; S. Frixione, Nucl. Phys. B **507** (1997) 295.

14. S. Catani and M. H. Seymour, Nucl. Phys. B **485** (1997) 291 [Erratum-ibid. B **510** (1997) 503].

15. D. A. Kosower, Phys. Rev. D **57** (1998) 5410, Phys. Rev. D **67** (2003) 116003, Phys. Rev. D **71** (2005) 045016.

16. S. Weinzierl, JHEP **0303** (2003) 062, JHEP **0307** (2003) 052.

17. S. Frixione and M. Grazzini, JHEP **0506** (2005) 010.

18. A. Gehrmann-De Ridder, T. Gehrmann and E. W. N. Glover, Phys. Lett. B **612** (2005) 36, Phys. Lett. B **612** (2005) 49, JHEP **0509** (2005) 056; A. Daleo, T. Gehrmann and D. Maitre, hep-ph/0612257.

19. G. Somogyi, Z. Trocsanyi and V. Del Duca, JHEP **0506** (2005) 024, JHEP **0701** (2007) 070; G. Somogyi and Z. Trocsanyi, JHEP **0701** (2007) 052.

20. A. Gehrmann-De Ridder, T. Gehrmann and E. W. N. Glover, Nucl. Phys. B **691** (2004) 195.

21. S. Weinzierl, Phys. Rev. D **74** (2006) 014020.

22. A. Gehrmann-De Ridder, T. Gehrmann, E. W. N. Glover and G. Heinrich, Nucl. Phys. Proc. Suppl. **160** (2006) 190.

23. A. Gehrmann-De Ridder, T. Gehrmann, E. W. N. Glover and G. Heinrich, JHEP **0712** (2007) 094 [arXiv:0711.4711 [hep-ph]].

24. S. Catani and M. Grazzini, Phys. Rev. Lett. **98** (2007) 222002 [arXiv:hep-ph/0703012].

25. M. Grazzini, JHEP **0802** (2008) 043 [arXiv:0801.3232 [hep-ph]].

26. S. Catani, D. de Florian and M. Grazzini, JHEP **0201** (2002) 015.

27. G. Parisi and R. Petronzio, Nucl. Phys. B **154** (1979) 427.

28. J. C. Collins, D. E. Soper and G. Sterman, Nucl. Phys. B **250** (1985) 199.

29. S. Catani, D. de Florian and M. Grazzini, Nucl. Phys. B **596** (2001) 299.

30. G. Bozzi, S. Catani, D. de Florian and M. Grazzini, Phys. Lett. B **564** (2003) 65, Nucl. Phys. B **737** (2006) 73, Nucl. Phys. B **791** (2008) 1.

31. M. Grazzini, JHEP **0601** (2006) 095.

32. D. de Florian and M. Grazzini, Phys. Rev. Lett. **85** (2000) 4678, Nucl. Phys. B **616** (2001) 247.

33. S. Catani, M. Grazzini, to appear.

34. D. de Florian, M. Grazzini and Z. Kunszt, Phys. Rev. Lett. **82** (1999) 5209; see also J. Campbell and R.K. Ellis, *MCFM - Monte Carlo for FeMtobarn processes*, `http://mcfm.fnal.gov`.

35. A. D. Martin, R. G. Roberts, W. J. Stirling and R. S. Thorne, Phys. Lett. B **604** (2004) 61.

36. CMS collaboration, *CMS Physics, Technical Design Report, Vol. II Physics Performance*, report CERN/LHCC 2006-021.

37. S. Catani and B. R. Webber, JHEP **9710** (1997) 005.

38. G. Davatz, G. Dissertori, M. Dittmar, M. Grazzini and F. Pauss, JHEP **0405** (2004) 009.

39. S. Catani, Y. L. Dokshitzer, M. H. Seymour and B. R. Webber, Nucl. Phys. B **406** (1993) 187; S. D. Ellis and D. E. Soper, Phys. Rev. D **48** (1993) 3160.

40. C. Anastasiou, G. Dissertori and F. Stockli, JHEP **0709** (2007) 018.

41. `http://theory.fi.infn.it/grazzini/codes.html`